

AD-A197 666

DTIC FILE COPY

4

AD

TECHNICAL REPORT ARCCB-TR-88030

A SIMPLE ANALYSIS OF THE  
SWAGE AUTOFRETTAGE PROCESS

PETER C. T. CHEN

DTIC  
-LECTE  
AUG 19 1988  
S D  
D C

JULY 1988



US ARMY ARMAMENT RESEARCH,  
DEVELOPMENT AND ENGINEERING CENTER  
CLOSE COMBAT ARMAMENTS CENTER  
BENÉT LABORATORIES  
WATERVLIET, N.Y. 12189-4050



APPROVED FOR PUBLIC RELEASE; DISTRIBUTION UNLIMITED

88 8 19 88

ADA197666

REPORT DOCUMENTATION PAGE		READ INSTRUCTIONS BEFORE COMPLETING FORM
1. REPORT NUMBER ARCCB-TR-88030	2. GOVT ACCESSION NO.	3. RECIPIENT'S CATALOG NUMBER
4. TITLE (and Subtitle) A SIMPLE ANALYSIS OF THE SWAGE AUTOFRETTAGE PROCESS		5. TYPE OF REPORT & PERIOD COVERED Final
7. AUTHOR(s) Peter C. T. Chen		6. PERFORMING ORG. REPORT NUMBER
9. PERFORMING ORGANIZATION NAME AND ADDRESS US Army ARDEC Benet Laboratories, SMCAR-CCB-TL Watervliet, NY 12189-4050		8. CONTRACT OR GRANT NUMBER(s)
11. CONTROLLING OFFICE NAME AND ADDRESS US Army ARDEC Close Combat Armaments Center Picatinny Arsenal, NJ 07806-5000		10. PROGRAM ELEMENT, PROJECT, TASK AREA & WORK UNIT NUMBERS AMCMS No. 6126.24.1BLO.OAR PRON No. 1A72ZH7QNMSC
14. MONITORING AGENCY NAME & ADDRESS (if different from Controlling Office)		12. REPORT DATE July 1988
		13. NUMBER OF PAGES 14
		15. SECURITY CLASS. (of this report) UNCLASSIFIED
16. DISTRIBUTION STATEMENT (of this Report)  Approved for public release; distribution unlimited.		15a. DECLASSIFICATION/DOWNGRADING SCHEDULE
17. DISTRIBUTION STATEMENT (of the abstract entered in Block 20, if different from Report)		
18. SUPPLEMENTARY NOTES Presented at the Fifth Army Conference on Applied Mathematics and Computing, U.S. Military Academy, West Point, New York, 15-18 June 1987. Published in Proceedings of the Conference.		
19. KEY WORDS (Continue on reverse side if necessary and identify by block number) Gun Tube Swaging Autofrettage Plasticity Residual Stress Bauschinger Effect Hardening		
20. ABSTRACT (Continue on reverse side if necessary and identify by block number) Many solutions have been reported for the hydraulic autofrettage process. In this report a simple analysis of the swage autofrettage process is presented. The contact pressure at different locations is determined as a function of interference. The deformation and stress distribution during autofrettage is obtained. At the end of the autofrettage process, the permanent bore enlargement and residual stresses are calculated. Numerical results are presented in graphical form.		

TABLE OF CONTENTS

	<u>Page</u>
INTRODUCTION	1
ELASTIC SWAGING	1
SWAGING BEYOND THE ELASTIC LIMIT	3
UNLOADING ANALYSIS	4
NUMERICAL RESULTS AND DISCUSSIONS	5
REFERENCES	7

LIST OF ILLUSTRATIONS

1. Contact pressure and hoop stress at the interface as functions of interference for a section in zone 1.	8
2. Contact pressure and hoop stress at the interface as functions of interference for a section in zone 2.	9
3. Contact pressure and hoop stress at the interface as functions of interference for a section in zone 3.	10
4. The hoop stress distributions at three sections.	11
5. The distributions of residual hoop stresses at three sections.	12
6. The distributions of residual displacements at three sections.	13

Approved for	
MRS. G. W. B.	✓
Date: 12/1/51	□
By	
Date	
Approved by: Gages	
Date	Accepted by: Steel
A-1	

## INTRODUCTION

To increase the maximum pressure a cylinder can contain without plastic deformation and to enhance its fatigue life, residual stresses are often produced in cylinders through autofrettage (ref 1). Many solutions have been reported for the hydraulic autofrettage process (refs 2-6). The thick-walled cylinders were subjected to uniform internal pressure of sufficient magnitude to cause plastic deformation and then the pressure was removed.

A more economical way of producing residual stresses in thick-walled cylinders is the swage autofrettage process. This process is carried out by a swage, the diameter of which is greater than the inner diameter of the cylinder. This swage is driven through the cylinder from one end to the other. A rigorous analysis of this process is difficult. In this report a simple analysis of the swage autofrettage process is presented. The swage mandrel and the cylinder are made of tungsten carbide and steel, respectively. A two-dimensional plane-strain analysis is used to determine the contact pressure at different locations of the cylinder as a function of interference. The deformation and stress distribution during autofrettage are obtained. At the end of the autofrettage process, the permanent bore enlargement and residual stresses are calculated.

## ELASTIC SWAGING

The swage mandrel is assumed to be a short cylindrical bar driven through a long thick-walled cylinder from one end to the other. The diameter of the mandrel ( $2c$ ) is a constant, but the inner and outer diameters ( $2a$  and  $2b$ ) of the tube are variables. When the difference between  $c$  and  $a$  is positive, we have interference  $I$ . For small values of interference, the stress state in the

---

References are listed at the end of this report.

swaging assembly is elastic. The stresses and displacement in the tube are

$$\begin{aligned} \frac{\sigma_r}{\sigma_\theta} &= \frac{p}{1 - a^2/b^2} \left[ \frac{a^2}{b^2} \mp \frac{a^2}{r^2} \right] \\ \frac{u}{r} &= \frac{p/E}{1 - a^2/b^2} \left[ (1+\nu) \frac{a^2}{r^2} + (1-\nu-2\nu^2) \frac{a^2}{b^2} \right] \end{aligned} \quad (1)$$

and in the mandrel

$$\begin{aligned} \sigma_r &= \sigma_\theta = -p \\ u/r &= -(1-\nu_1-2\nu_1^2)p/E_1 \end{aligned} \quad (2)$$

where  $E$ ,  $\nu$ , and  $E_1$ ,  $\nu_1$  are the material constants of the tube and mandrel, respectively. At the interface,  $u_a$  (tube) -  $u_a$  (mandrel) =  $I$  by the compatibility requirement. The interference pressure  $p$  is a function of the interference  $I$  given by

$$p = \frac{EI}{a} \left( 1 - \frac{a^2}{b^2} \right) / \left[ (1+\nu) + (1-\nu-2\nu^2) \frac{a^2}{b^2} + (1-\nu_1-2\nu_1^2) \left( 1 - \frac{a^2}{b^2} \right) E/E_1 \right] \quad (3)$$

For sufficiently large values of the interference, the stresses in the tube reach the yield limit. Assuming that Tresca's yield condition governs the behavior of the material, the tube first becomes plastic at the interference when the stresses satisfy  $\sigma_\theta - \sigma_r = \sigma_0$ , where  $\sigma_0$  is the initial tensile yield stress. The solution for the critical interference pressure to cause incipient plastic deformation is

$$p^* = \frac{1}{2} \sigma_0 \left( 1 - a^2/b^2 \right) \quad (4)$$

and it follows from Eq. (3) that the interference for the onset of plastic flow is

$$I^* = \frac{\sigma_0}{E} \frac{a}{2} \left[ (1+\nu) + (1-\nu-2\nu^2) \frac{a^2}{b^2} + (1-\nu_1-2\nu_1^2) \left( 1 - \frac{a^2}{b^2} \right) E/E_1 \right] \quad (5)$$

which reduces to  $I^* = (1-\nu^2) a \sigma_0/E$  for the special case ( $E_1 = E$ ,  $\nu_1 = \nu$ ).

## SWAGING BEYOND THE ELASTIC LIMIT

For values of interference larger than that given by Eq. (5), a plastic zone forms in the tube, so that for  $a \leq r \leq \rho$  the tube is plastic, while for  $\rho \leq r \leq b$  the tube material is still in an elastic state. The elastic-plastic interface radius  $\rho$  is a function of the interference  $I$ .

We assume that the steel tube is elastically-ideally plastic, obeying Tresca's yield criterion and the associated flow theory, but the tungsten carbide mandrel is elastic. This assumption is justified because the strength ratio of tungsten carbide to steel is about three. For loading beyond the elastic limit, the closed-form solution has been found by Koiter (ref 2). The expressions for the stresses and displacement in the tube are

$$\begin{aligned} \frac{\sigma_r}{\sigma_0} &= \frac{1}{2} \left( 1 + \frac{\rho^2}{b^2} \right) - \log \frac{\rho}{r}, \quad \text{in } (a \leq r \leq \rho) \\ \frac{\sigma_\theta}{\sigma_0} & \end{aligned} \quad (6)$$

$$\begin{aligned} \frac{\sigma_r}{\sigma_0} &= \frac{1}{2} \left( \frac{\rho^2}{b^2} - \frac{\rho^2}{r^2} \right), \quad \text{in } (\rho \leq r \leq b) \\ \frac{\sigma_\theta}{\sigma_0} & \end{aligned} \quad (7)$$

$$\frac{E}{\sigma_0} \frac{u}{r} = (1-2\nu)(1+\nu) \frac{\sigma_r}{\sigma_0} + (1-\nu^2) \frac{\rho^2}{r^2} \quad (8)$$

where the elastic-plastic interface  $\rho$  is related to the internal pressure  $p$  by

$$p/\sigma_0 = \frac{1}{2} \left( 1 - \rho^2/b^2 \right) + \log(\rho/a) \quad (9)$$

For swaging beyond the elastic limit, the compatibility requires  $u_a$  (tube) -  $u_a$  (mandrel) =  $I$  at the interface, i.e.,

$$\frac{E}{\sigma_0} \frac{I}{a} = (1-\nu^2) \frac{\rho^2}{a^2} - \frac{\rho}{\sigma_0} \left[ (1-2\nu)(1+\nu) - (1-\nu_1-2\nu_1^2) \frac{E}{E_1} \right] \quad (10)$$

Equations (9) and (10) give us a parametric representation of relating  $p$  to  $I$  through the parameter  $\rho$ . The contact pressure at different locations can thus be determined as a function of the interference  $I$ .

## UNLOADING ANALYSIS

After swaging, the permanent bore enlargement and residual stresses can be calculated by an unloading analysis. Let a double prime denote a component in the residual state, i.e.,  $\sigma_{\theta}'' = \sigma_{\theta} + \sigma_{\theta}'$ . Assuming elastic unloading, the solution is given by

$$\begin{aligned} \sigma_r' \\ \sigma_{\theta}' \end{aligned} = \frac{p}{b^2/a^2 - 1} \left[ \pm \frac{b^2}{r^2} - 1 \right] \quad (11)$$

$$E u'/r = - [(1-\nu) + (1+\nu)b^2/r^2]p/(b^2/a^2-1) \quad (12)$$

In a recent paper (ref 6), this author presented a more rigorous elastic-plastic unloading analysis based on a new theoretical model considering the Bauschinger and hardening effects during unloading. This mode is a very good representation for the material behavior of the high strength steel used in gun tubes (ref 7). Taking into account the Bauschinger effect ( $f$ ) and the strain-hardening during unloading ( $m'$ ), we have obtained a closed-form solution. On unloading, yielding will occur for  $a \leq r < \rho'$  with  $\rho' < \rho$ . The stresses in the reverse yielding zone ( $a \leq r < \rho'$ ) are given by

$$\sigma_r'/\sigma_0 = p/\sigma_0 - \frac{1}{2}\beta_2'(1+f)(\rho'/a)^2(1-a^2/r^2) - (1-\beta_2')(1+f)\log(r/a) \quad (13)$$

$$\sigma_{\theta}'/\sigma_0 = \sigma_r'/\sigma_0 - (1+f)[1 + \beta_2'(\rho'^2/r^2-1)] \quad (14)$$

where

$$\beta_1' = (1-m')/[m' + \frac{\sqrt{3}}{2} \frac{(1-m')}{(1-\nu^2)}] \quad , \quad \beta_2' = m'\beta_1'/(1-m') \quad (15)$$

The stresses in the elastic zone ( $\rho' \leq r \leq b$ ) are

$$\begin{aligned} \sigma_r'/\sigma_0 \\ \sigma_{\theta}'/\sigma_0 \end{aligned} = \frac{1}{2}(1+f) \left[ \pm (\rho'/r)^2 - (\rho'/b)^2 \right] \quad (16)$$

The displacement for the entire tube ( $a \leq r \leq b$ ) is

$$(E\sigma_0)u'/r = (1-2\nu)(1+\nu)(\sigma_r'/\sigma_0) - (1-\nu^2)(1+f)(\rho'/r)^2 \quad (17)$$

The residual stresses and displacement are found by addition

$$\sigma_r'' = \sigma_r + \sigma_r' \quad , \quad \sigma_\theta'' = \sigma_\theta + \sigma_\theta' \quad \text{and} \quad u'' = u + u' \quad (18)$$

#### NUMERICAL RESULTS AND DISCUSSION

The material constants used in the calculations are  $E = 206.84$  GPa,  $\nu = 0.3$ ,  $\sigma_0 = 1.29$  GPa,  $m' = 0.3$  for the high strength steel, and  $E_1 = 610.19$  GPa,  $\nu_1 = 0.258$  for the tungsten carbide mandrel. The radius of the mandrel is a constant  $c = 58.42$  mm, but the thickness of the tube varies along the axial direction with the inner radius ( $a$ ) increasing slightly and the external radius ( $b$ ) tapering more rapidly. The values of  $a$  and  $b$  at four typical sections are  $a_j = 56.96, 57.82, 57.99, 58.63$  mm and  $b_j = 157.50, 106.75, 83.00, 83.00$  mm, for  $j = 1, 2, 3, 4$ , respectively. The corresponding values of wall ratio are  $b_j/a_j = 2.765, 1.846, 1.431, 1.42$  at four sections. The interference during swaging ( $I$ ) is the positive difference between  $c$  and  $a$ . The values of  $I$  at four sections are  $I_j = 1.46, 0.60, 0.43, -0.21$  mm for  $j = 1, 2, 3, 4$ . The negative value of  $I_4$  means that there is no contact between the mandrel and the tube. For the positive values of interference, the contact pressure and the stress distribution during swaging can be obtained using the methods presented previously in this report. The information after swaging can be obtained by the unloading analysis also presented previously.

The numerical results are presented in terms of the dimensionless quantities defined by

$$\begin{aligned} \bar{r} &= r/a \quad , \quad \bar{p} = p/\sigma_0 \quad , \quad \bar{\sigma}_\theta = \sigma_\theta/\sigma_0 \\ \bar{I} &= (E/\sigma_0)I/a \quad , \quad \bar{u} = (E/\sigma_0)u/a \quad , \quad \text{etc.} \end{aligned} \quad (19)$$

The contact pressure ( $\bar{p}$ ) and hoop stress ( $\bar{\sigma}_\theta$ ) at the interface are presented as functions of the interference ( $\bar{I}$ ) in Figures 1, 2, and 3 for wall ratios  $b/a =$

2.765, 1.846, 1.431, respectively. The results for swaging within and beyond the elastic limit are included. The pressure is a monotonous increasing function of the interference, but the maximum value of hoop stress occurs at the onset of plastic flow as shown in the dotted curves. Initial yielding occurs at  $\bar{I}^* = 0.774, 0.799, 0.830$ , and fully plastic flow occurs at  $\bar{I}^{**} = 6.638, 2.909, 1.751$  for three different wall ratios, respectively. The actual values of interference ( $\bar{I}$ ) at the three chosen sections are  $\bar{I}_1 = 4.10, \bar{I}_2 = 1.66, \bar{I}_3 = 1.19$ . These values indicate that swaging is partially plastic at these sections in zones 1, 2, and 3. The corresponding locations of elastic-plastic boundary are given by  $\rho/a = 2.2001, 1.4196, 1.19205$ , and the amounts of overstrain are 68, 49.6, and 44.6 percent, respectively. Also shown in Figures 1, 2, and 3 are the values of contact pressure ( $\bar{p} = 0.972, 0.555, 0.671$ ) and the hoop stress at the interface  $\bar{\sigma}_\theta = 1 - \bar{p}$ . The distributions of hoop stresses during swaging are shown in Figure 4 for typical sections in three zones. The maximum value of hoop stress occurs at the elastic-plastic boundary. The information for the displacement and stresses after swaging can be obtained by an unloading analysis. The distributions of residual hoop stresses are shown in Figure 5 for the chosen sections in three zones. Elastic unloading analysis is justified in zone 3, but reverse yieldings occur in zones 1 and 2 with  $\rho'/a = 1.305$  and  $1.014$ , respectively. Finally, the distributions of residual displacements ( $\bar{u}''$ ) at typical sections in three zones are presented in Figure 6. Also shown in this figure are the experimental data at the bore. The agreement between the calculated and experimental data is excellent in zone 1, but not so good in zones 2 and 3. This suggests that a more refined analysis is needed for sections with smaller wall ratios. An investigation based on the finite element method is being conducted and the results will be reported in the near future.

## REFERENCES

1. Davidson, T.E. and Kendall, D.P., "The Design of Pressure Vessels for Very High Pressure Operation," Mechanical Behavior of Materials Under Pressure, (H.L.P. Pugh, ed.), Elsevier Co., 1970.
2. Hill, R., The Mathematical Theory of Plasticity, Oxford University Press, London, 1950.
3. Bland, D.R., "Elastoplastic Thick-Walled Tubes of Work-Hardening Materials Subject to Internal and External Pressures and Temperature Gradients," Journal of Mechanics and Physics of Solids, Vol. 4, 1956, pp. 209-229.
4. Franklin, G.J. and Morrison, J.L.M., "Autofrettage of Cylinders: Prediction of Pressure/External Expansion Curves and Calculation of Residual Stresses," Proceedings of the Institute of Mechanical Engineers, Vol. 174, 1960, pp. 947-974.
5. Chen, P.C.T., "The Finite Element Analysis of Elastic-Plastic Thick-Walled Tubes," Proceedings of Army Symposium on Solid Mechanics, The Role of Mechanics in Design-Ballistic Problems, 1972, pp. 243-253.
6. Chen, P.C.T., "The Bauschinger and Hardening Effect on Residual Stresses in an Autofrettaged Thick-Walled Cylinder," Journal of Pressure Vessel Technology, Vol. 108, February 1986, pp. 108-112.
7. Milligan, R.V., Koo, W.H., and Davidson, T.E., "The Bauschinger Effect in a High Strength Steel," Journal of Basic Engineering, Vol. 88, June 1966, pp. 480-488.

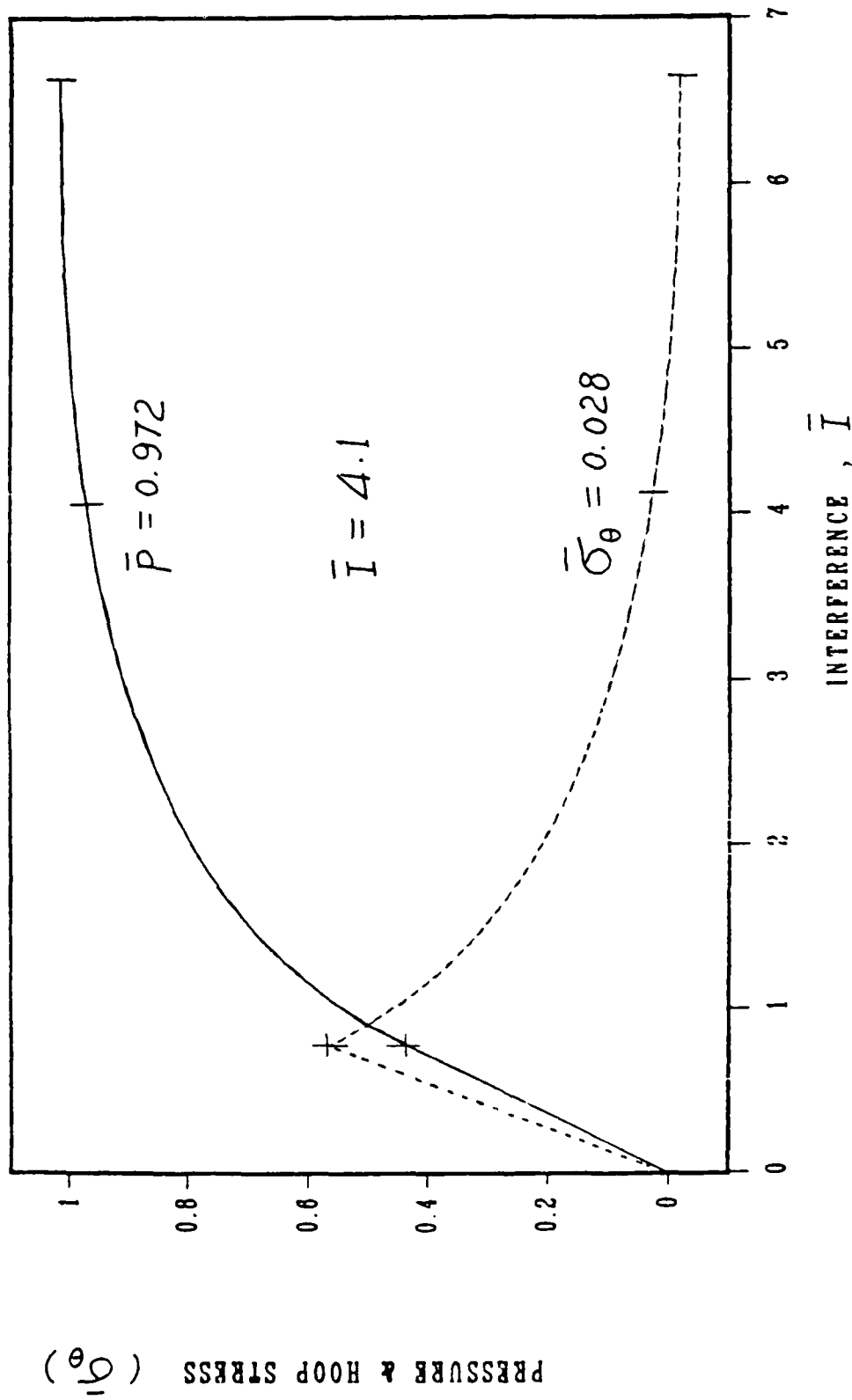


Figure 1. Contact pressure and hoop stress at the interface as functions of interference for a section in zone 1.

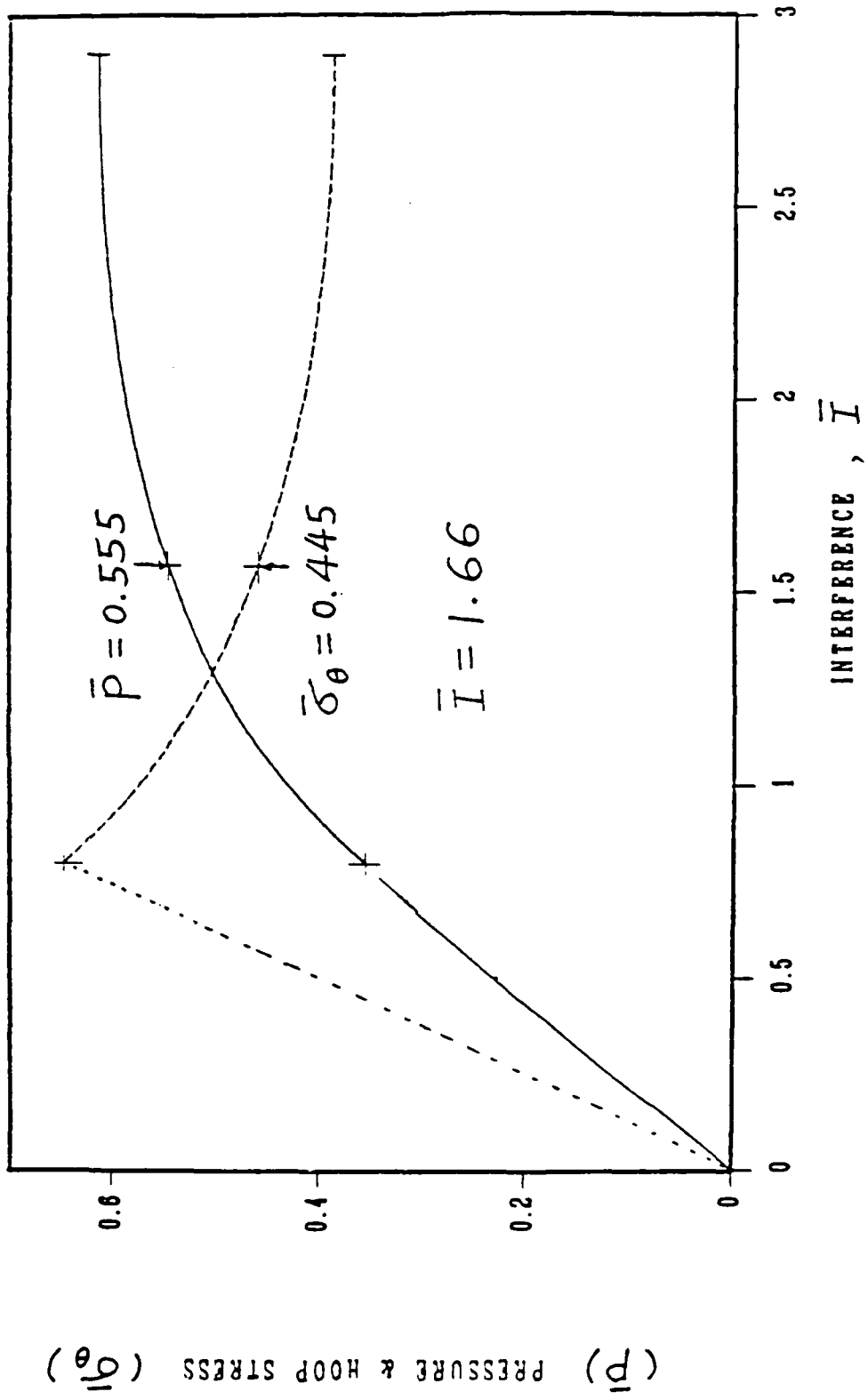


Figure 2. Contact pressure and hoop stress at the interface as functions of interference for a section in zone 2.

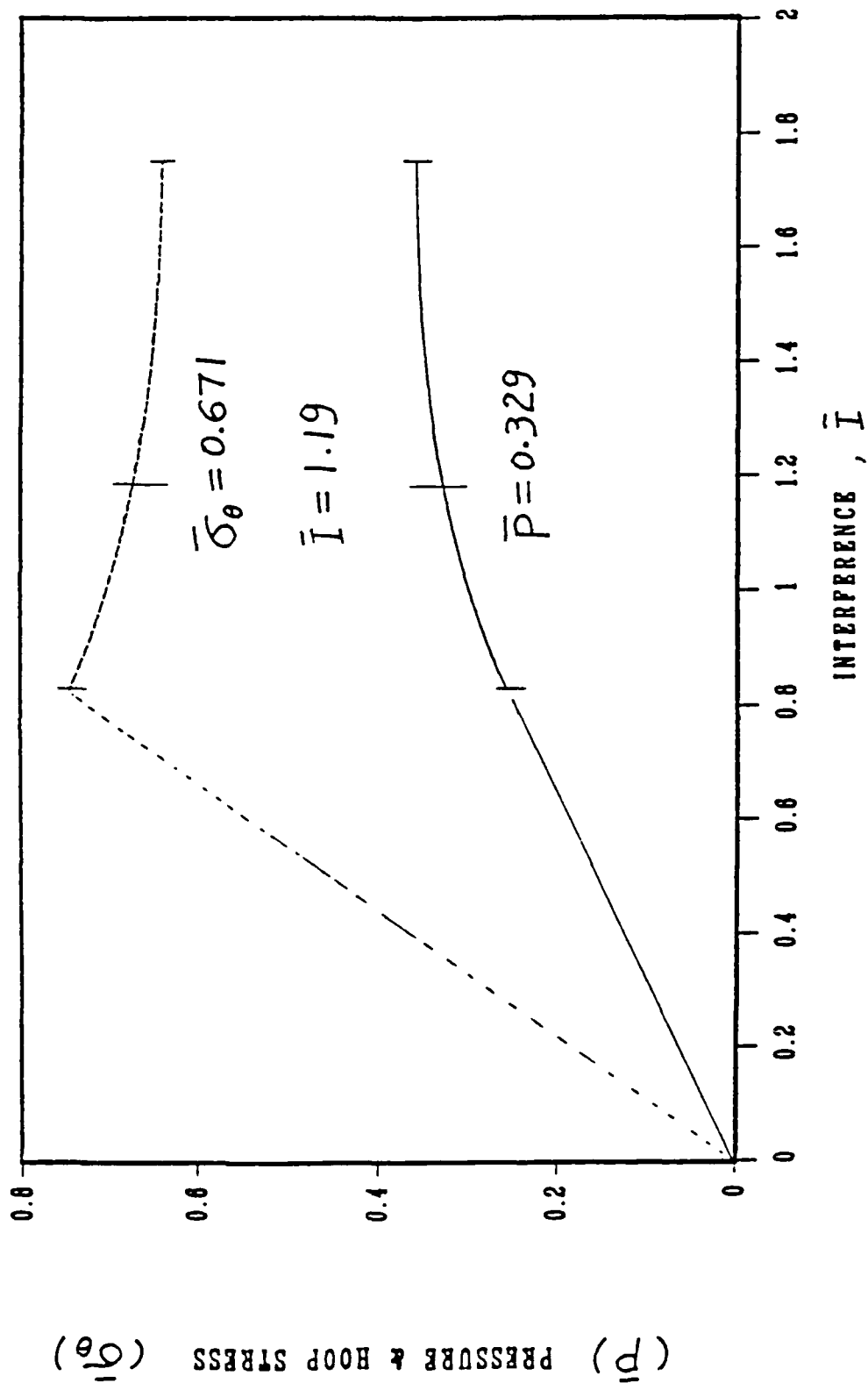


Figure 3. Contact pressure and hoop stress at the interface as functions of interference for a section in zone 3.

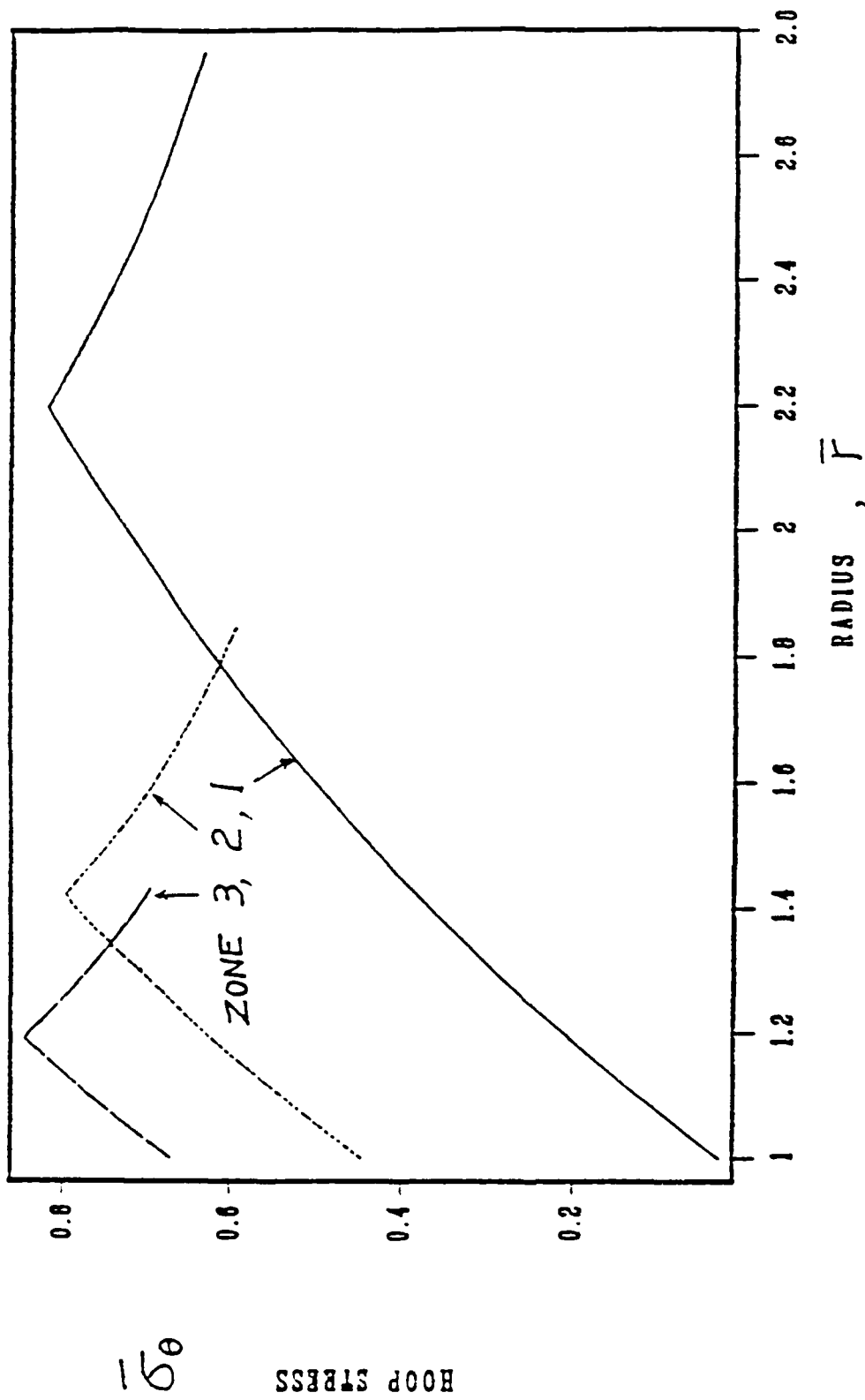


Figure 4. The hoop stress distributions at three sections.

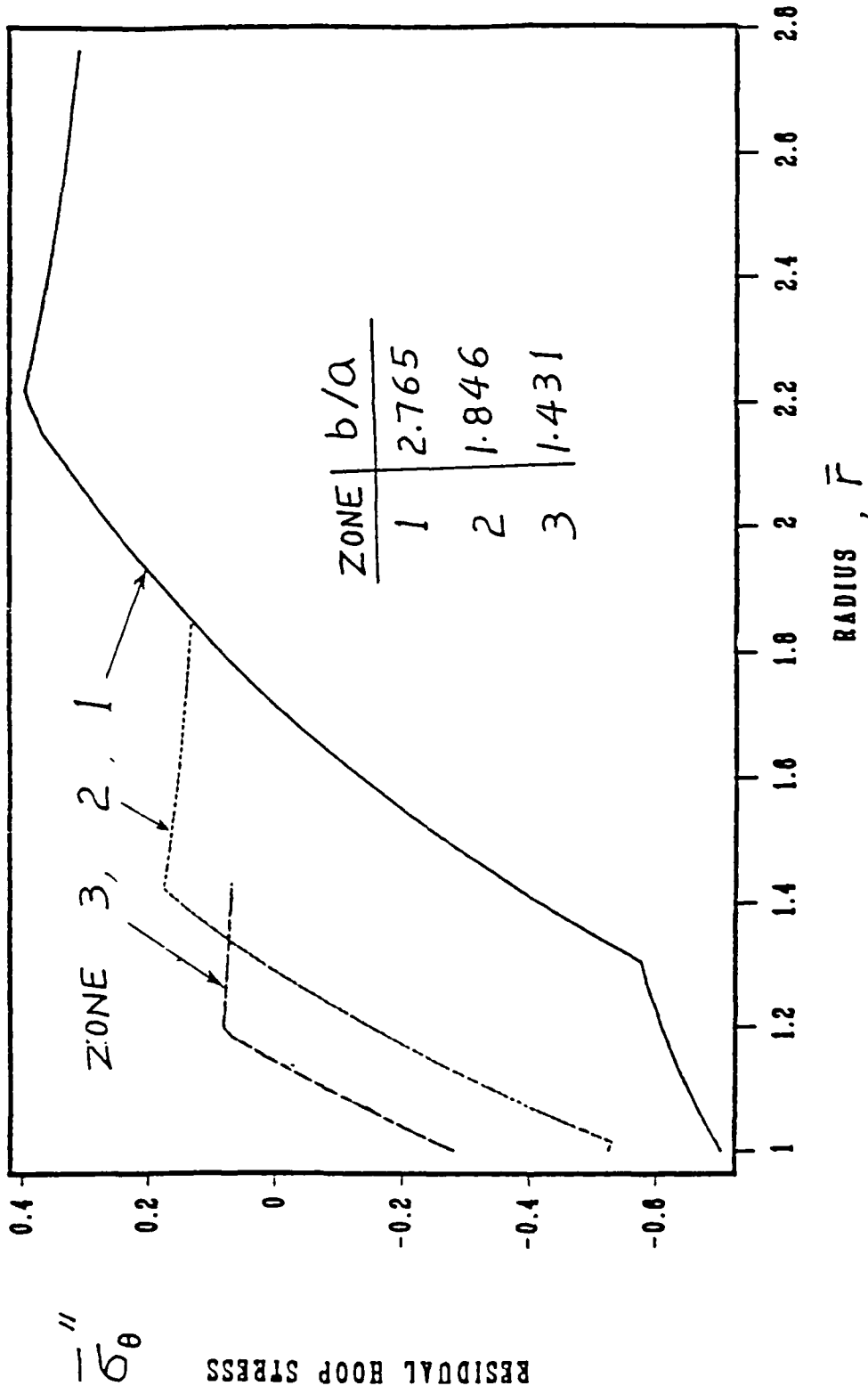


Figure 5. The distributions of residual hoop stresses at three sections.

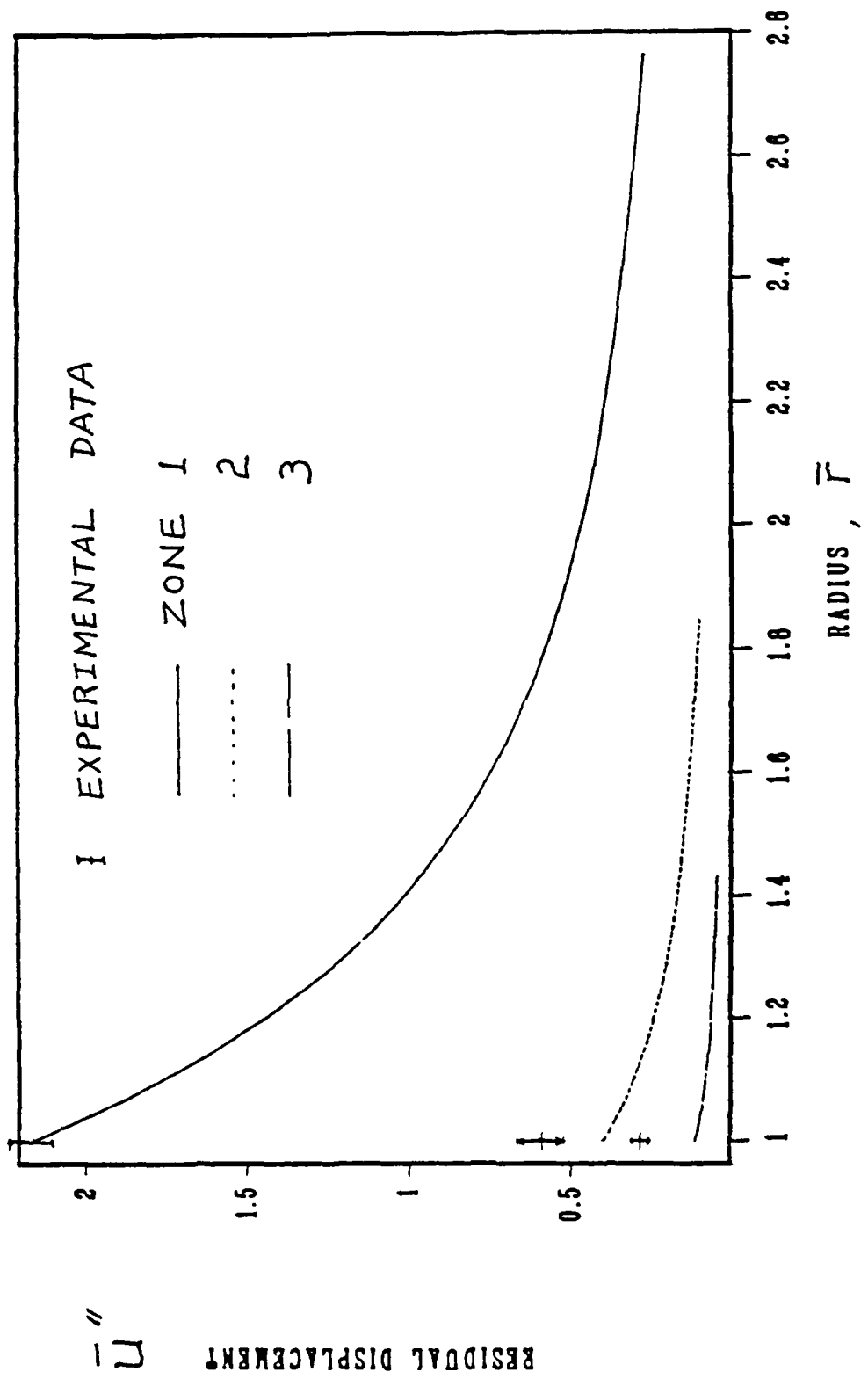


Figure 6. The distributions of residual displacements at three sections.

TECHNICAL REPORT INTERNAL DISTRIBUTION LIST

	<u>NO. OF COPIES</u>
CHIEF, DEVELOPMENT ENGINEERING BRANCH	
ATTN: SMCAR-CCB-D	1
-DA	1
-DC	1
-DM	1
-DP	1
-DR	1
-DS (SYSTEMS)	1
CHIEF, ENGINEERING SUPPORT BRANCH	
ATTN: SMCAR-CCB-S	1
-SE	1
CHIEF, RESEARCH BRANCH	
ATTN: SMCAR-CCB-R	2
-R (ELLEN FOGARTY)	1
-RA	1
-RM	1
-RP	1
-RT	1
TECHNICAL LIBRARY	
ATTN: SMCAR-CCB-TL	5
TECHNICAL PUBLICATIONS & EDITING UNIT	
ATTN: SMCAR-CCB-TL	2
DIRECTOR, OPERATIONS DIRECTORATE	
ATTN: SMCWV-OD	1
DIRECTOR, PROCUREMENT DIRECTORATE	
ATTN: SMCWV-PP	1
DIRECTOR, PRODUCT ASSURANCE DIRECTORATE	
ATTN: SMCWV-QA	1

NOTE: PLEASE NOTIFY DIRECTOR, BENET LABORATORIES, ATTN: SMCAR-CCB-TL, OF ANY ADDRESS CHANGES.

TECHNICAL REPORT EXTERNAL DISTRIBUTION LIST

	<u>NO. OF COPIES</u>		<u>NO. OF COPIES</u>
ASST SEC OF THE ARMY RESEARCH AND DEVELOPMENT ATTN: DEPT FOR SCI AND TECH THE PENTAGON WASHINGTON, D.C. 20310-0103	1	COMMANDER ROCK ISLAND ARSENAL ATTN: SMCRI-ENM ROCK ISLAND, IL 61299-5000	1
ADMINISTRATOR DEFENSE TECHNICAL INFO CENTER ATTN: DTIC-FDAC CAMERON STATION ALEXANDRIA, VA 22304-6145	12	DIRECTOR US ARMY INDUSTRIAL BASE ENGR ACTV ATTN: AMXIB-P ROCK ISLAND, IL 61299-7260	1
COMMANDER US ARMY ARDEC ATTN: SMCAR-AEE	1	COMMANDER US ARMY TANK-AUTMV R&D COMMAND ATTN: AMSTA-DDL (TECH LIB) WARREN, MI 48397-5000	1
SMCAR-AES, BLDG. 321	1	COMMANDER	
SMCAR-AET-O, BLDG. 351N	1	US MILITARY ACADEMY	1
SMCAR-CC	1	ATTN: DEPARTMENT OF MECHANICS	
SMCAR-CCP-A	1	WEST POINT, NY 10996-1792	
SMCAR-FSA	1		
SMCAR-FSM-E	1	US ARMY MISSILE COMMAND	
SMCAR-FSS-D, BLDG. 94	1	REDSTONE SCIENTIFIC INFO CTR	2
SMCAR-IMI-I (STINFO) BLDG. 59	2	ATTN: DOCUMENTS SECT, BLDG. 4484	
PICATINNY ARSENAL, NJ 07806-5000		REDSTONE ARSENAL, AL 35898-5241	
DIRECTOR US ARMY BALLISTIC RESEARCH LABORATORY ATTN: SLCBR-DD-T, BLDG. 305	1	COMMANDER US ARMY FGN SCIENCE AND TECH CTR ATTN: DRXST-SD	1
ABERDEEN PROVING GROUND, MD 21005-5066		220 7TH STREET, N.E. CHARLOTTESVILLE, VA 22901	
DIRECTOR US ARMY MATERIEL SYSTEMS ANALYSIS ACTV ATTN: AMXSY-MP	1	COMMANDER US ARMY LABCOM	
ABERDEEN PROVING GROUND, MD 21005-5071		MATERIALS TECHNOLOGY LAB	
COMMANDER HQ, AMCCOM		ATTN: SLCMT-IML (TECH LIB)	2
ATTN: AMSMC-IMP-L	1	WATERTOWN, MA 02172-0001	
ROCK ISLAND, IL 61299-6000			

NOTE: PLEASE NOTIFY COMMANDER, ARMAMENT RESEARCH, DEVELOPMENT, AND ENGINEERING CENTER, US ARMY AMCCOM, ATTN: BENET LABORATORIES, SMCAR-CCB-TL, WATERVLIET, NY 12189-4050, OF ANY ADDRESS CHANGES.

TECHNICAL REPORT EXTERNAL DISTRIBUTION LIST (CONT'D)

	<u>NO. OF COPIES</u>		<u>NO. OF COPIES</u>
COMMANDER US ARMY LABCOM, ISA ATTN: SLCIS-IM-TL 2800 POWDER MILL ROAD ADELPHI, MD 20783-1145	1	COMMANDER AIR FORCE ARMAMENT LABORATORY ATTN: AFATL/MN EGLIN AFB, FL 32542-5434	1
COMMANDER US ARMY RESEARCH OFFICE ATTN: CHIEF, IPO P.O. BOX 12211 RESEARCH TRIANGLE PARK, NC 27709-2211	1	COMMANDER AIR FORCE ARMAMENT LABORATORY ATTN: AFATL/MNF EGLIN AFB, FL 32542-5434	1
DIRECTOR US NAVAL RESEARCH LAB ATTN: MATERIALS SCI & TECH DIVISION CODE 26-27 (DOC LIB) WASHINGTON, D.C. 20375	1 1	METALS AND CERAMICS INFO CTR BATTELLE COLUMBUS DIVISION 505 KING AVENUE COLUMBUS, OH 43201-2693	1

NOTE: PLEASE NOTIFY COMMANDER, ARMAMENT RESEARCH, DEVELOPMENT, AND ENGINEERING CENTER, US ARMY AMCCOM, ATTN: BENET LABORATORIES, SMCAR-CCB-TL, WATERVLIET, NY 12189-4050, OF ANY ADDRESS CHANGES.

END

DATE

FILMED

DTIC

9-88